Biointerface Research in Applied Chemistry
Open-Access Journal (ISSN: 2069-5837)

Article
Volume 13, Issue 2, 2023, 101
https://doi.org/10.33263/BRIAC132.101

Conjugation of Curcumin and Metformin for Improved Pharmacological Profile in Cancer Therapy: An *In Silico* Approach

Vijaybhanu Perumalsamy [1,*], Harish Kumar D R [1], Sarasija Suresh [2]

[1] Department of Pharmaceutical Chemistry, Faculty of Pharmacy, M.S. Ramaiah University of Applied Sciences, Bengaluru 560032, Karnataka, India; vijaybhanu.p@gmail.com (V.P); drhkshs@gmail.com (H.K.D.R);
[2] Institute for Drug Delivery and Biomedical Research, Bengaluru 560086, Karnataka, India.; sarasija_s@hotmail.com (S.S);
* Correspondence: vijaybhanu.p@gmail.com (V.P);

Scopus Author ID 57220194099
Received: 27.12.2021; Accepted: 24.01.2022; Published: 20.02.2022

Abstract: Curcumin has been shown to possess high cytotoxicity towards various cell lines. But its low aqueous solubility and bioavailability limit its use as an effective cytotoxic agent. It has been reported that metformin selectively kills cancer stem cells and blocks tumor growth. Preclinical studies show the effectiveness of both curcumin and metformin in breast cancer. Conjugation of metformin and curcumin may result in synergistic cancer therapy by improving the aqueous solubility of curcumin and hence its bioavailability. In the present study, curcumin-metformin conjugate and the free drugs curcumin and metformin were subjected to docking analysis against the breast cancer targets such as epidermal growth factor receptor, kinesin spindle protein, cyclin-dependent kinase, human placental aromatase, and human estrogen receptor. Docking studies were performed using Autodock Vina. The results signify that curcumin-metformin conjugate showed higher binding energy ranging between -7.4 to -9.7 Kcal/mol than curcumin and metformin. The stability of the conjugate-receptor complex and interactions between them was further evaluated by molecular dynamics simulation. The results showed that the conjugate can interact effectively with human placental aromatase and can be considered for further studies.

Keywords: curcumin; metformin; conjugation; drug-drug conjugate; docking; breast cancer.

1. Introduction

Cancer is one of the most common causes of disease-related deaths worldwide, accounting for about 10 million deaths in 2020 [1]. Breast cancer is the most frequent type among women and is the second major cause of high incidence of death. According to the estimates provided by GLOBOCAN, female breast cancer has overtaken lung cancer as the most often diagnosed cancer in the year 2020 worldwide [2,3]. Current predictions and statistics show that the incidence of breast cancer and the related mortality rate is on the rise [4]. Many chemotherapeutic drugs have been developed that inhibit the uncontrolled cell division process to treat different types of cancer. But there is a need to develop effective anti-cancer drugs despite the number of drugs in clinical use due to the high prevalence of adverse effects and multidrug resistance [5].

Epidermal growth factor receptor (EGFR) is overexpressed in about half of all triple-negative and inflammatory breast cancer (TNBC and IBC) patients. It is a crucial target for the development of new anti-cancer drugs. TNBC and IBC patients may benefit from EGFR targeted treatment [6]. Overexpression of the motor protein-kinesin spindle protein (KSP) has been demonstrated as an important therapeutic target of breast cancer [7]. KSP inhibitors may prevent the mitotic spindle formation during cell division, inducing the breast cancer cells to apoptosis [8]. Cyclin-dependent kinase (CDK) prevents the over-proliferation of breast cancer cells. It has been suggested that CDK inhibition may be a viable therapeutic target to develop anti-cancer drugs [9,10]. Estrogen plays a major role in breast cancer, and the aromatase enzyme synthesizes estrogen from androgen. Aromatase inhibitors are prominent drugs in estrogen-dependent breast cancer therapy[11]. Over half of breast cancer cases overexpress estrogen receptor alpha. There is increasing evidence for estrogen antagonists that reduce estrogen biosynthesis as efficient therapeutic agents in breast cancer [12].

Curcumin is a promising anti-cancer agent exhibiting multi-potent properties and activities against a number of molecular targets *in vitro* [13,14]. *In vitro* and *in vivo* studies demonstrated that curcumin acts as an antiangiogenic, anti-invasive, and antimetastatic agent [15]. It was reported to inhibit cell proliferation in breast cancer and induce apoptosis [16]. Translation of curcumin into a drug for treatment is restricted by its poor oral bioavailability due to poor solubility and extensive pre-systemic and systemic metabolism [17,18]. Recent studies indicated that the antidiabetic drug metformin shows great potential in cancer management [19]. Based on epidemiological research, metformin inhibits the mammalian target of rapamycin-dependent translation initiation in breast cancer cells [20]. The synergistic activity of metformin and chemotherapeutic drugs specifically targeting breast cancer stem cells has been reported in *in vitro* and *in vivo* models [21,22]. Drug-drug conjugation is a novel approach to create conjugates with complementary therapeutic activities increased bioavailability and thus may result in synergistic activity, increased absorption, reduced dose, and toxicity [23]. Conjugation of metformin and curcumin could prevent the pre-systemic intestinal metabolism of curcumin and thus may enhance the oral bioavailability of both drugs.

Virtual screening has been an efficient approach for discovering and developing new drug candidates. Molecular docking studies aid in identifying the lead candidates so that only potent compounds can be screened experimentally. In this study, the binding effectiveness of curcumin-metformin conjugate was investigated against the breast cancer targets by *in silico* approach.

2. Materials and Methods

2.1. Protein structure preparation.

The X-ray crystal structures of epidermal growth factor receptor tyrosine kinase (PDB: 1M17), kinesin spindle protein (PDB: 1Q0B), cyclin-dependent kinase (PDB: 1YKR), human placental aromatase (PDB: 3S7S), and human estrogen receptor (PDB: 2IOK) were obtained from the Research Collaboratory for Structural Bioinformatics (RCSB) Protein Data Bank [24]. The target protein was prepared by inserting the missing residues using Swiss-PDB v4.1.0. The file was saved in pdb format and utilized for further studies.

2.2. Ligand structure preparation.

Ligand structure preparation is essential to produce a single, energetically stable structure with accurate spatial orientation and stereochemistry. This increases the chances of obtaining potential hit molecules at the end of the drug discovery process. The molecular structure of curcumin-metformin conjugate (CON) was drawn using Chemdraw. The 3D structures of curcumin, metformin, and other standard drugs were downloaded from PubChem and saved in SDF format in a docking workspace file. The chemical structures of curcumin, metformin, and conjugate are given in Figure 1. A ligand cluster was created, and their energies were minimized.

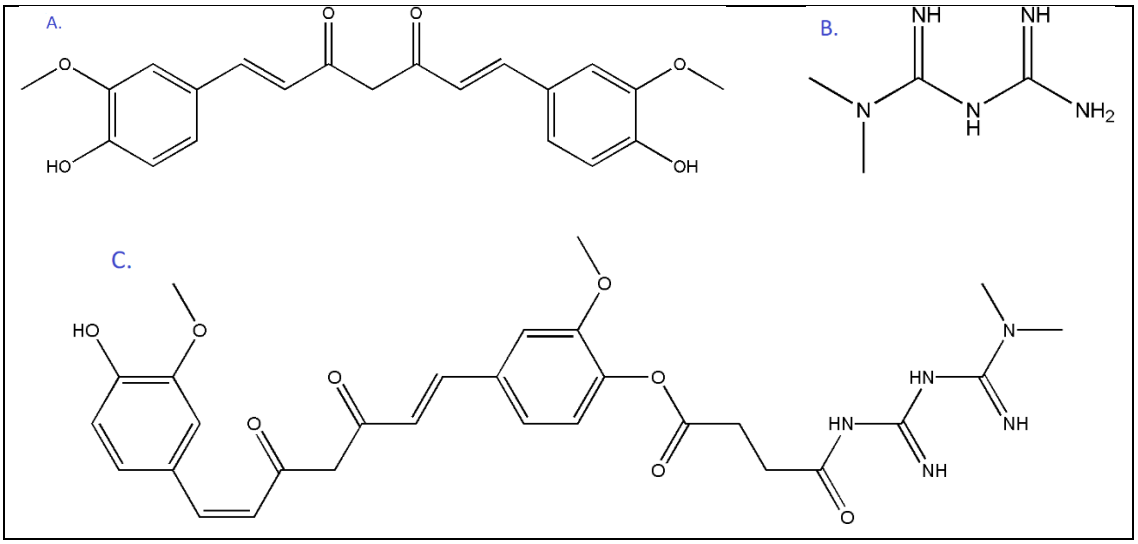

Figure 1. Chemical structures of ligands. **A**. Curcumin, **B**. Metformin, **C**. Curcumin-Metformin conjugate.

2.3. Docking protocol.

Docking of protein and ligands was carried out using Autodock Vina, inbuilt in PyRx software [25-27]. The ligands were assumed to be flexible and the protein as rigid during the docking process. The configuration file for the grid parameters was generated with dimensions (A°) of x=59.27, y=51.29, z=25.00 for IM17; x=25.35, y=14.06, z=76.16 for 1Q0B; x=18.36, y=18.03, z=19.85 for 1YKR; x=87.34, y=53.72, z=25.00 for 3S7S and x=29.98, y=21.70, z=25.00 for 2IOK. The protein and ligand structures were saved in 'pdbqt' format for calculating the binding affinities. The amino acid residues at the active site of a protein that interacts with the ligands were identified. The best ligand was chosen based on its binding affinity with the respective target protein at the active site. Discovery Studio Visualizer was used for visualizing the interactions between the ligand and protein [28].

2.4. ADMET analysis.

The ligands were further subjected to predicting pharmacokinetic properties such as absorption, distribution, metabolism, excretion, and toxicity (ADMET) using the pkCSM web server [29].

The structures of curcumin, metformin, and conjugate structures were converted to SMILE structures and used for predicting pharmacokinetics. The parameters such as water solubility, Caco-2 intestinal permeability, human skin permeability, steady-state distribution volume, blood-brain barrier permeability, CNS permeability, metabolic interactions with

cytochromes, total renal clearance, and toxicity were measured determined using pkCSM software.

2.5. Molecular dynamics.

The binding stability and the interactions between conjugate and the receptor human placental aromatase were evaluated by molecular dynamics (MD) simulation. The ligand-receptor complex file was subjected to MD simulations using GROMACS tool version 2021.3 [30-32]. Ligand topologies were selected from PRODRG server [33]. The processed setup was vacuum minimized for 500 steps by applying the steepest descent method. A simple point charge (SPC) water model was used to solve complex structures in a cubic periodic box of 0.5 nm. Subsequently, Na^+ and Cl^- counter ions were added to the solvated system to obtain an appropriate salt concentration of 0.15 M. Then, each resultant structure from NPT (Isothermal-Isobaric, constant number of particles, pressure, and temperature) equilibration phase was subjected for the final run in NPT ensemble for a simulation time of 100 ns. The obtained trajectory data was analyzed using the GROMACS simulation package through the online server WebGRO for macromolecular simulations (https://simlab.uams.edu/) to understand root mean square deviation (RMSD), root mean square fluctuation (RMSF), radius of gyration (Rg) and solvent accessible surface area (SASA). Molecular Mechanics Poisson–Boltzmann Surface Area (MMPBSA) analysis was utilized to calculate the binding free energy of the protein-ligand complex. A GROMACS tool g_mmpbsa was used to estimate the binding free energies [34].

3. Results and Discussion

Molecular docking studies of curcumin, metformin, and the conjugate was performed with five target proteins such as epidermal growth factor receptor tyrosine kinase, kinesin spindle protein, cyclin-dependent kinase, human placental aromatase, and human estrogen receptor to understand the molecular basis of interaction and affinity of binding of these ligands with the proteins. The ranking of the compounds was based on their binding energy with the enzyme.

The docking results of the ligands with protein EGFR are given in Table 1, and the interaction images are shown in Figure 2. The docking score of the conjugate was found to be -8.4 Kcal/mol while for the standard drug Erlotinib -6.9 Kcal/mol. Among the ligands, the conjugate exhibited the best docking score. The conjugate forms conventional hydrogen bonding with GLN-767, LYS-721, MET-769, attractive charge interaction with ASP-831, carbon hydrogen bonding GLU-738, pi-sigma interactions with VAL-702 and pi-alkyl interaction with ARG-817 at the active site of protein.

The docking results of the ligands with protein KSP are given in Table 2. The conjugate showed the best docking score of -8.8 Kcal/mol compared to the other two ligands and the standard drug Monastrol. The conjugate forms a conventional hydrogen bond with PHE-113, THR-112, GLY-108, LYS-111, LEU-266, SER-235, and attractive charge interaction with ASP-265 active site of protein as shown in Figure 3.

Table 1. Binding affinity and interactions of ligands against EGFR.

Ligand	Docking score	Binding interactions
Curcumin	-7.4	Conventional hydrogen bond-GLN A:767,THR A:766; Pi-Cation-LYS A:721; Pi-Sigma-LEU A:820; Pi-Sulphur-MET A:742; Alkyl and Pi-Alkyl-CYS A:751, LYS A:721, ALA A:719, VAL A:702; van

Ligand	Docking score	Binding interactions
		der Waals-MET A:769, LEU A:694, LEU A:768, THR A:830, ASP A:831, PHE A:699, ILE A:720, GLU A:738, LEU A:753, LEU A:764
Metformin	-4.7	van der Waals-ALA A:719, LEU A:768, VAL A:702, LEU A:820, THR A:766, LYS A:721, CYS A:751, THR A:830, MET A:742, ASP A:831; Carbon Hydrogen bond-GLU A:738, Conventional hydrogen bond-GLN A:767
Curcumin-Metformin conjugate	-8.4	van der Waals-ASP A:776, MET A:742, CYS A:751, THR A:830, ALA A:719, LEU A:768, LEU A:694, GLY A:695, GLY A:772, PHE A:699, ASN A: 818; Conventional Hydrogen bond: GLN A:767, LYS A:721, MET A:769; Attractive charge-ASP A:831, Carbon Hydrogen bond: GLU A:738; Pi-Sigma-VAL A:702; Pi-Alkyl-ARG A:817
Erlotinib	-6.9	van der Waals-THR A:830, ASP A:831, PHE A:699, GLY A:695, CYS A:773, THR A:766, LEU A:820, ALA A:719, LEU A:768, PRO A:770; Conventional hydrogen bond-MET A:769; Carbon-Hydrogen bond-GLY A:772; Pi-Cation-LYS A:721; Pi-Sigma-LEU A:694; Pi-Alkyl-LEU A:764, VAL A:702

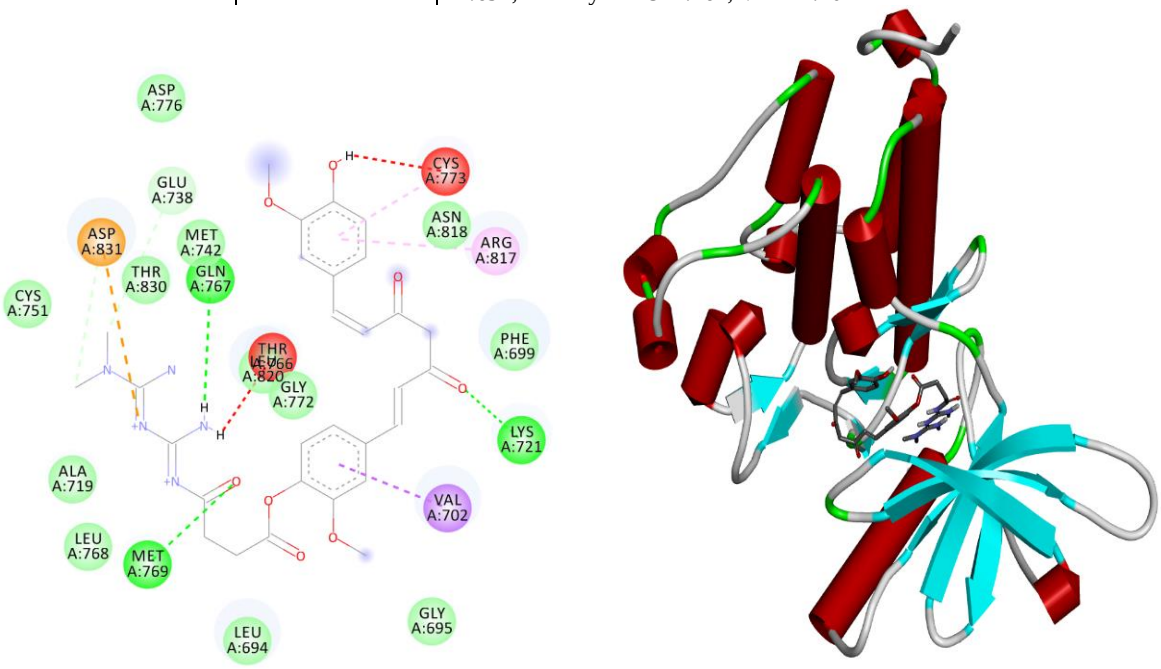

Figure 2. Binding interaction between curcumin-metformin conjugate and EGFR - 2D (left) and 3D (right) representation.

Table 2. Binding affinity and interactions of the ligands against KSP.

Ligand	Docking score	Binding interactions
Curcumin	-7.4	Conventional hydrogen bond-GLU A:116; Pi-Alkyl-ALA A:218, LEU A:214, ILE A:136; Carbon Hydrogen bond-ALA A:133; van der Waals-THR A:112, TYR A:211, TRP A:127, PRO A:137,SER A:237,PHE A:239, LEU A:160, GLU A:118, GLY A:117, ARG A:119, GLY A:134
Metformin	-5.9	van der Waals-THR B:112, LYS B:111, GLU B:116, LEU B:266, ALA B:267, HIS B:236, GLY B:268, SER B:233, ARG B:221, TYR B:231; Carbon Hydrogen bond-GLU B:162, Conventional hydrogen bond-SER B:232, SER B:235; Attractive charge-ASP B:265
Curcumin-Metformin conjugate	-8.8	van der Waals-GLU A:118, GLY A:110, ARG A:221, SER A:237, SER A:232, PRO A:27, ARG A:26, PHE A:28, ASN A:29, SER A:233, GLY A:268, ALA A:267, HIS A:236; Conventional Hydrogen bond: PHE A:113, THR A:112, GLY A:108, LYS A:111, LEU A:266, SER A:235; Attractive charge-ASP A:265
Monastrol	-7.8	van der Waals-TRP A:127, ALA A:133, GLY A:217, ALA A:218, THR A:112, GLU A:118; Conventional hydrogen bond-LEU A:214, GLU A:116, GLY A:117; Carbon-Hydrogen bond-GLU A:116; Alkyl and Pi-Alkyl-TYR A:211, PRO A:137, ILE A:136, ARG A:119

The docking results of the ligands with protein CDK are given in Table 3, and the binding interactions are shown in Figure 4. The conjugate exhibited the best docking score of -9.2 Kcal/mol compared to the free drugs and the standard 5-fluoro uracil. It forms the following binding interactions with the amino acid residues of the protein- conventional hydrogen bonding with LEU-83, THR-14, LYS-129, ASP-86; alkyl and pi-alkyl interactions with PHE-80, LYS-33, ALA-144, VAL-18, ILE-10; carbon-hydrogen bonding with ASP-145 and pi-cation interaction with GLU-8.

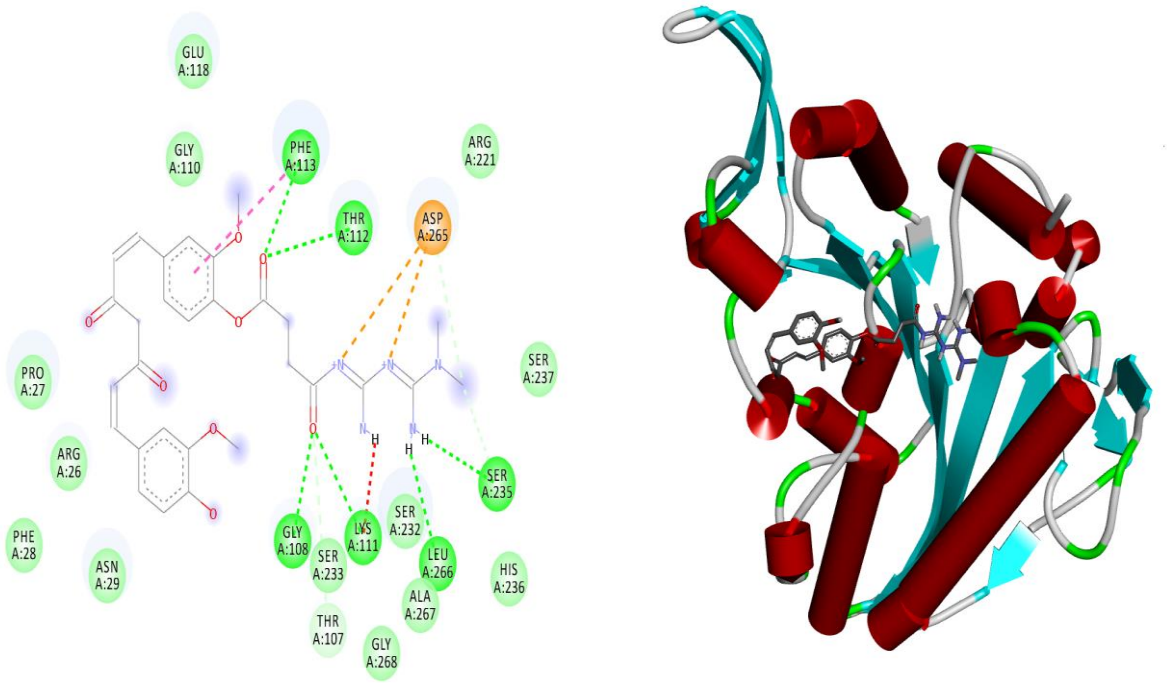

Figure 3. Binding interaction between curcumin-metformin conjugate and KSP - 2D (left) and 3D (right) representation.

Table 3. Binding affinity and interactions of the ligands against CDK.

Ligand	Docking score	Binding interactions
Curcumin	-8.2	Conventional hydrogen bond-LEU A:83; Carbon Hydrogen bond-ASN A:132; Pi-Sigma-VAL A:18; Pi-Alkyl-ALA A:31, LYS A:33; van der Waals-GLN A:85, LEU A:134, PHE A:82, ASP A:86, GLN A:131, GLY A:13, ILE A:10, GLY A:11, GLU A:12, PHE A:80, LEU A: 148, ASP A:145
Metformin	-4.7	van der Waals- LEU A:134, LYS A:129, GLY A:13, ALA A:31, THR A:14, VAL A:18, TYR A:15, LYS A:33, PHE A:80; Attractive charge-ASP A:145, Conventional hydrogen bond-GLN A:131, ASA A:132
Curcumin-Metformin conjugate	-9.2	van der Waals-LYS A:20, HIS A:84, PHE A:82, LYS A:89, GLU A:81, ALA A:31, GLY A:11, ASN A:132, LEU A:134, GLN A:131, GLY A:13, GLU A:12; Conventional Hydrogen bond-LEU A:83, THR A:14, LYS A:129, ASP A:86; Alkyl and Pi-Alkyl-PHE A:80, LYS A:33, ALA A:144, VAL A:18, ILE A:10; Carbon hydrogen bond-ASP A:145; Pi-cation-GLU A:8
5-Fluoro uracil	-4.9	van der Waals-LEU A:148, LYS A:33, VAL A:64, LEU A:134, ILE A:10; Conventional hydrogen bond-ASP A:145; Pi-Pi-stacked-PHE A:80; Pi-Alkyl-ALA A:144, VAL A:18, ALA A:31

The docking results of the ligands with protein human placental aromatase and human estrogen receptor are given in Tables 4 and 5. Among the docked ligands, the conjugate showed a better docking score of -9.7 Kcal/mol and -8.8 Kcal/mol with aromatase and estrogen receptor, respectively, compared to the free drugs. The conjugate forms conventional hydrogen bonding with THR-310, CYS-437, MET-374, ARG-115; pi-pi-T shaped interactions with TRP-224; pi-alkyl interactions with VAL-370, LEU-477 for aromatase receptor and

conventional hydrogen bonding with LEU-346; attractive charge interaction with ASP-351, carbon hydrogen bonding with LEU-387; pi-sigma interactions with LEU-525; pi-sulfur interactions with ASP -351; alkyl and pi-alkyl interactions with LEU-391 and ALA-350 for estrogen receptor as shown in Figure 5 and 6.

Table 4. Binding affinity and interactions of the ligands against human placental aromatase.

Ligand	Docking score	Binding interactions
Curcumin	-8.3	Conventional hydrogen bond-ARG A:115, LEU A:372; Pi-Sulphur-MET A:374; Pi-Pi-T shaped-PHE A:134, Alkyl and Pi-Alkyl-ALA A:438, CYS A:437, ILE A:133, LEU A:477, VAL A:370, VAL A:373; van der Waals-ILE A:132, ARG A:145,GLY A:436, ARG A:435, PHE A:430, PHE A:221, ALA A:306, ILE A:305, ASP A:309, TRP A:224, THR A:310
Metformin	-4.4	van der Waals-SER A:199, ALA A:306, PHE A:203, MET A:160, THR A:310, LEU A:152, MET A:446, ILE A:442, GLY A:439, ALA A:443, CYS A:437; Conventional hydrogen bond-MET A:303
Curcumin-Metformin conjugate	-9.7	van der Waals-PHE A:148, LEU A:152, ILE A:132, ALA A:438, GLY A:439, ALA A:443, ILE A:133, ALA A:306, MET A:311, PHE A:134, VAL A:369, SER A:478, PHE A:221, ASP A:309, VAL A: 373, LEU A:372; Conventional Hydrogen bond-THR A:310, CYS A:437, MET A:374, ARG A:115; Pi-Pi-T shaped-TRP A:224; Pi-Alkyl-VAL A:370, LEU A:477
Exemestane	-9.6	van der Waals-LEU A:372, PHE A:134, LEU A:477, SER A:478, TRP A:224, THR A:310, ILE A:305, VAL A:373, ILE A:133; Conventional hydrogen bond-MET A:374, ARG A:115; Carbon-Hydrogen bond-ALA A:306; Alkyl and Pi-Alkyl-VAL A:370, PHE A:221

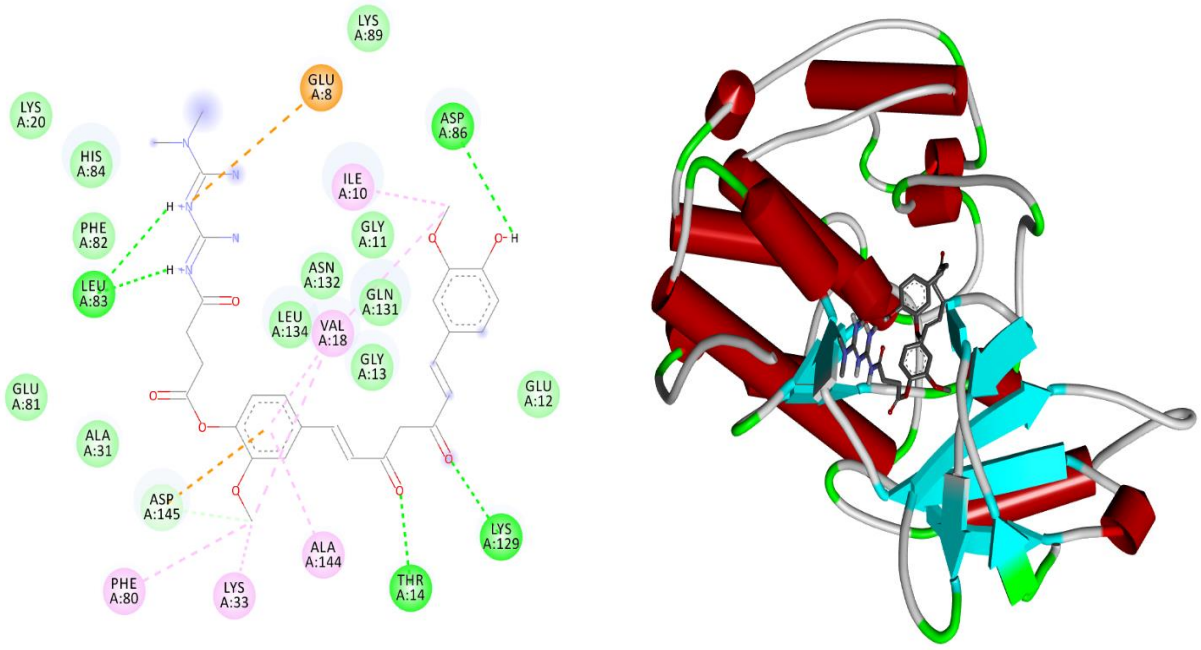

Figure 4. Binding interaction between curcumin-metformin conjugate and CDK - 2D (left) and 3D (right) representation.

Table 5. Binding affinity and interactions of the ligands against human estrogen receptor.

Ligand	Docking score	Binding interactions
Curcumin	-8.3	Conventional hydrogen bond-THR A:347, GLY A:521; Pi-Sulphur-MET A:421; Alkyl and Pi-Alkyl-ALA A:350, TRP A:383, LEU A:525, HIS A:524, ILE A:424; Amide-Pi stacked-LEU A:346; van der Waals-LEU A:354, LEU A:387, ARG A:394, GLU A:353, PHE A:404, MET A:388, LEU A:391, LEU A:384, LEU A:428, GLY A:420
Metformin	-5.1	van der Waals-PRO A:325, HIS A:356, ARG A:394, PHE A:445, MET A:357, TRP A:393, PRP A:324, LYS A:449, LEU A:387, ILE A:386, ILE A:326; Carbon Hydrogen bond-GLY A:390, Conventional hydrogen bond-GLU A:353; Attractive charge-GLU A:353

Curcumin-Metformin conjugate	-8.8	van der Waals-HIS A:524, ILE A:424, MET A:421, LEU A:428, MET A:388, LEU A:384, ARG A:394, GLU A:353, LEU A:349, TRP A:383, LEU A:354, LEU A:539; Conventional Hydrogen bond: LEU A:346; Attractive charge-ASP A:351, Carbon Hydrogen bond: LEU A:387; Pi-Sigma-LEU A:525; Pi-Sulphur-ASP A:351; Alkyl and Pi-Alkyl-LEU A:391, ALA A:350
Tamoxifen	-9.6	van der Waals-ARG A:394, GLU A:353, LEU A:349, ASP A:351, TRP A:383, GLY A:521, ILE A:424, HIS A:524, MET A:388, LEU A:384, LEU 354; Carbon-Hydrogen bond-THR A:347; Pi-Sulphur-MET A:421; Pi-Sigma-LEU A:387; Pi-Pi stacked-PHE A:404; Alkyl and Pi-Alkyl-LEU A:391, LEU A:428, LEU A:525, ALA A:350, LEU A:346

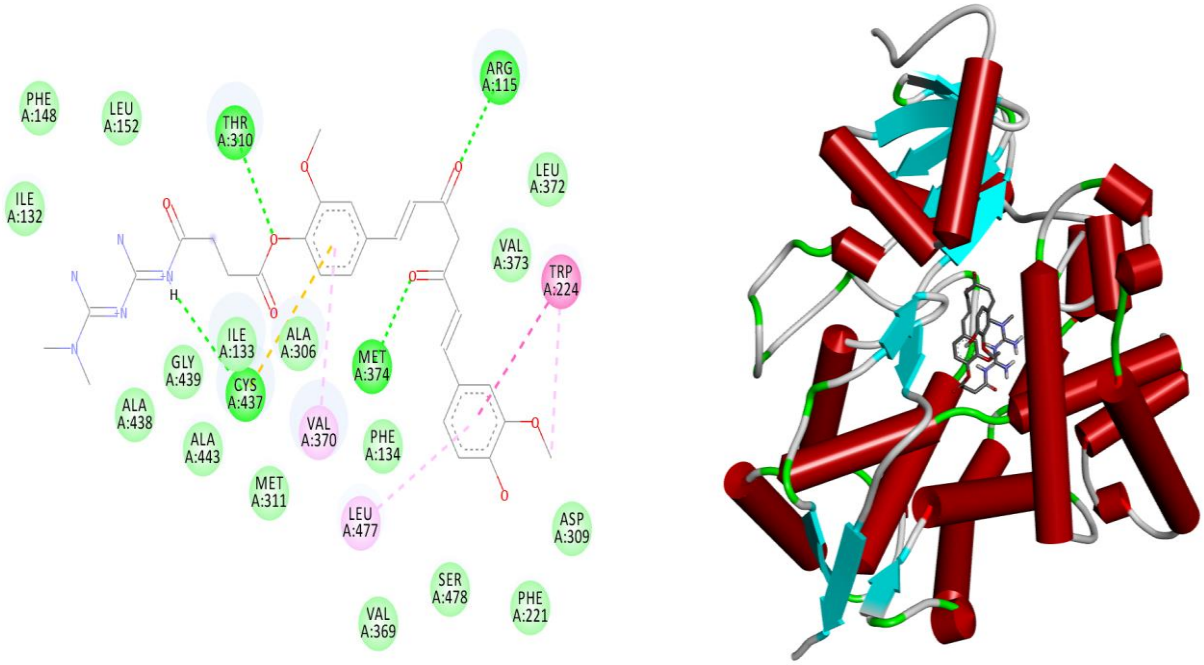

Figure 5. Binding interaction between curcumin-metformin conjugate and human placental aromatase - 2D (left) and 3D (right) representation.

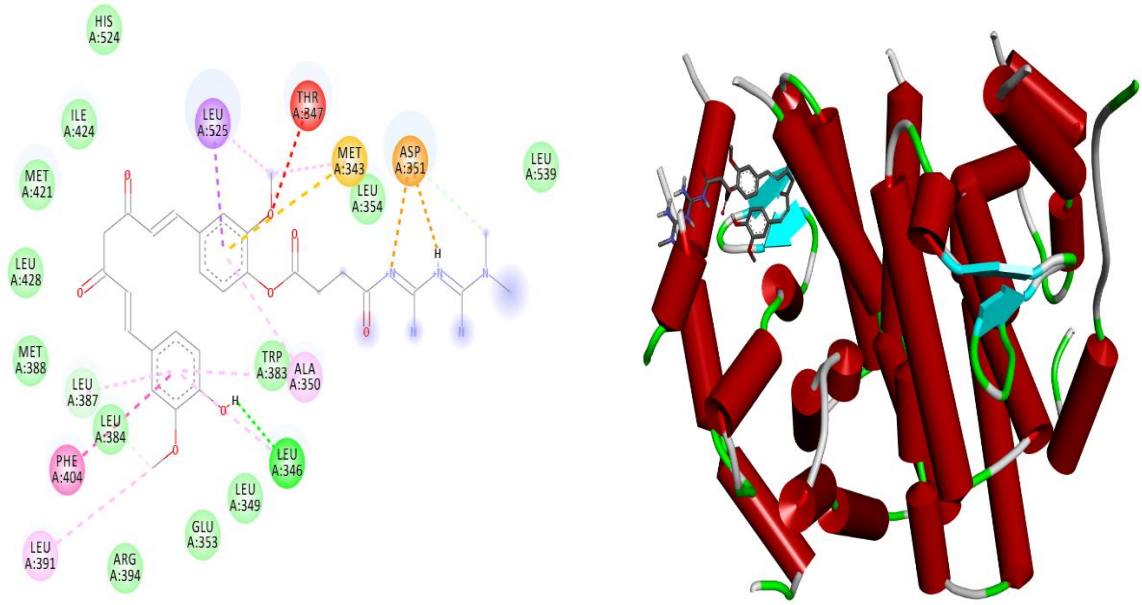

Figure 6. Binding interaction between curcumin-metformin conjugate and human estrogen receptor - 2D (left) and 3D (right) representation.

Among the target proteins, curcumin-metformin conjugate interacted well with the human placental aromatase enzyme (3S7S), showing the maximum docking score of -9.7 Kcal/mol, which is close to that of standard drug exemestane with the docking score of -9.6 Kcal/mol. This suggests that the inhibitory effect of the conjugate on the aromatase enzyme may be the possible mechanism of action. The identification of molecular interactions and the binding positions of docking protein-ligand complexes revealed that the conjugate was able to produce the binding interactions consisting of van der Waals, hydrogen, and pi-bonds, indicating that these interactions may be essential for inhibition of the enzyme.

The results of predicted ADMET properties are shown in Table 6. *In silico* prediction demonstrated that the conjugate has better water solubility (-2.894 log mol/L) than curcumin (-4.194 log mol/L), which is close to that of metformin (-2.707 log mol/L). The conjugate and the free drugs showed low Caco-2 intestinal permeability, blood-brain barrier, and CNS permeability. As per the data obtained, all the compounds are predicted to have good skin permeability as their log Kp values are less than -2.5. The three ligands were observed to be substrates of P-glycoprotein, indicating that the transport and excretion of these compounds is dependent on the P-glycoprotein pathway. The analysis revealed that the conjugate and the free drugs were not human OCT2 substrates, which is essential for the excretion of cationic molecules. *In silico* prediction shows that the conjugate is excreted moderately through kidneys (0.647 log mL/min/kg) with a low steady-state volume of distribution. The interactions of conjugate and human cytochrome systems were predicted to understand its metabolic pathway and compared with free drugs. No interactions with major human cytochromes are predicted for both conjugate and metformin. The conjugate is predicted to be devoid of cardiotoxicity as free drugs. The results also suggest that the conjugate may not be toxic in AMES test and may not have hepatotoxicity and skin sensitization.

Table 6. Predicted ADMET properties of compounds.

Properties	**Compounds**		
	Curcumin	**Metformin**	**Curcumin-Metformin conjugate**
Water solubility(log mol/L)	-4.194	-2.707	-2.894
Caco2 permeability(log Papp in 10^{-6} cm/s)	0.322	-0.339	-0.28
Skin Permeability(log Kp)	-2.74	-2.735	-2.735
P-glycoprotein substrate	Yes	Yes	Yes
P-glycoprotein I inhibitor	Yes	No	Yes
P-glycoprotein II inhibitor	Yes	No	No
VDss (human)log L/kg))	-0.137	-0.232	-0.325
Fraction unbound (human)(Fu)	0.118	0.811	0.391
BBB permeability(log BB)	-0.374	-0.946	-2.253
CNS permeability(log PS)	-2.957	-4.238	-3.8
CYP2D6 substrate	No	No	No
CYP3A4 substrate	No	No	No
CYP1A2 inhibitor	No	No	No
CYP2C19 inhibitor	Yes	No	No
CYP2C9 inhibitor	Yes	No	No
CYP2D6 inhibitor	No	No	No
CYP3A4 inhibitor	Yes	No	No
Total Clearance(log ml/min/kg)	0.073	0.1	0.647
Renal OCT2 substrate	No	No	No
AMES toxicity	No	Yes	No
Max. tolerated dose (human) (log mg/kg/day)	0.16	0.902	0.378
hERG I inhibitor	No	No	No
Oral Rat Acute Toxicity (LD50) (mol/kg)	2.466	2.453	2.473

Properties	Compounds		
	Curcumin	Metformin	Curcumin-Metformin conjugate
Oral Rat Chronic Toxicity (LOAEL) (log mg/kg_bw/day)	1.725	2.158	3.797
Hepatotoxicity	No	No	No
Skin Sensitisation	No	Yes	No
T.pyriformis toxicity(log ug/L)	0.36	0.25	0.285
Minnow toxicity(log mM)	-0.328	3.972	1.689

The conjugate is predicted to have better water solubility and is devoid of toxicity from the above-observed results. So it may have sufficient potential to be a drug, but further experimental studies are required to substantiate the data.

The apo form of human placental aromatase protein (PDB: 3S7S) along with the complex of the conjugate, curcumin, and standard exemestane were further analyzed to study the binding stability of the protein-ligand complex. MD simulations were performed to assess the structural and conformational changes of three complexes for a simulation time of 100 ns. The stability and fluctuations of these complexes were examined by analyzing the parameters such as RMSD, RMSF, Rg, and SASA of receptor atoms.

RMSD is an indicator to analyze the stability of the complexes [35]. RMSD of the protein backbone atoms was plotted against time to analyze its changes in structural conformations. Apo form of the protein showed stable conformation from 30 ns until the end of the simulation. In the case of the conjugate, stable conformation was attained from 20 ns. For curcumin, stable conformation was attained from 40 ns but showed slight fluctuation in the stability. In the case of standard, stable conformation was shown from 30 ns. RMSD study plot is shown in Figure 7.

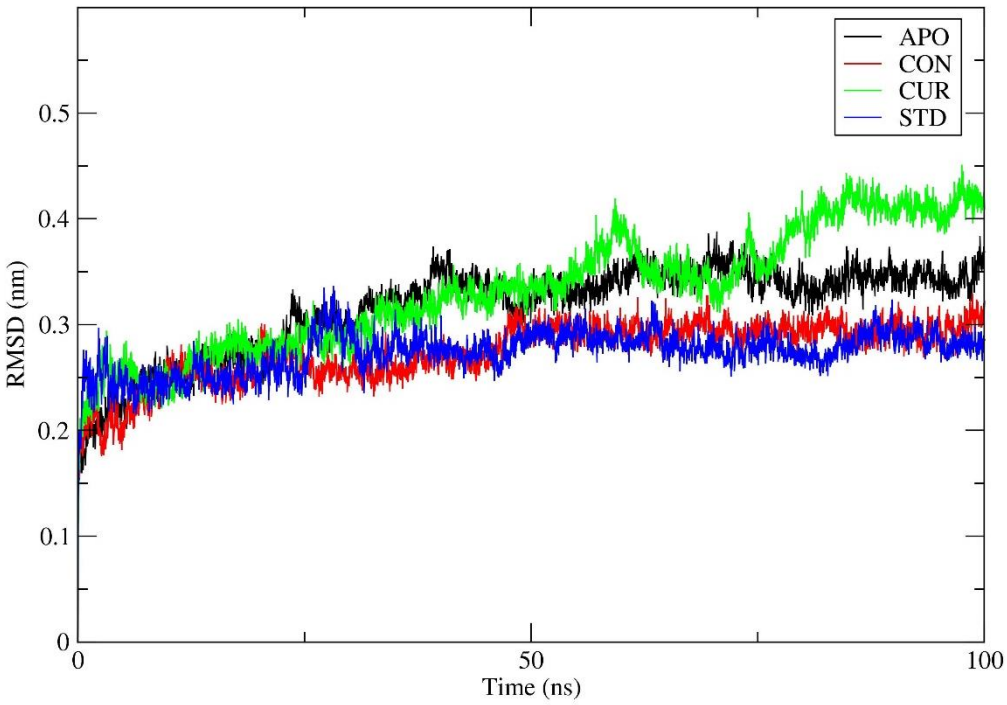

Figure 7. Study plot of RMSD of 3S7S-APO (Black), 3S7S-CON (Red), 3S7S-Curcumin (Green), and 3S7S-Standard (Blue) for 100 ns MD simulation.

RMSF was analyzed for conjugate bound complex and the apo form and standard exemestane complex to evaluate the flexibility of the amino acid residues of target protein on binding to a ligand. The RMSF values for C**α** atoms of the protein were calculated and plotted against the residues as shown in Figure 8. In the case of each complex, the amino acid residues

showed minor variations during the simulation. The results show that binding of the ligands had no significant influence on the flexibility of the protein residues.

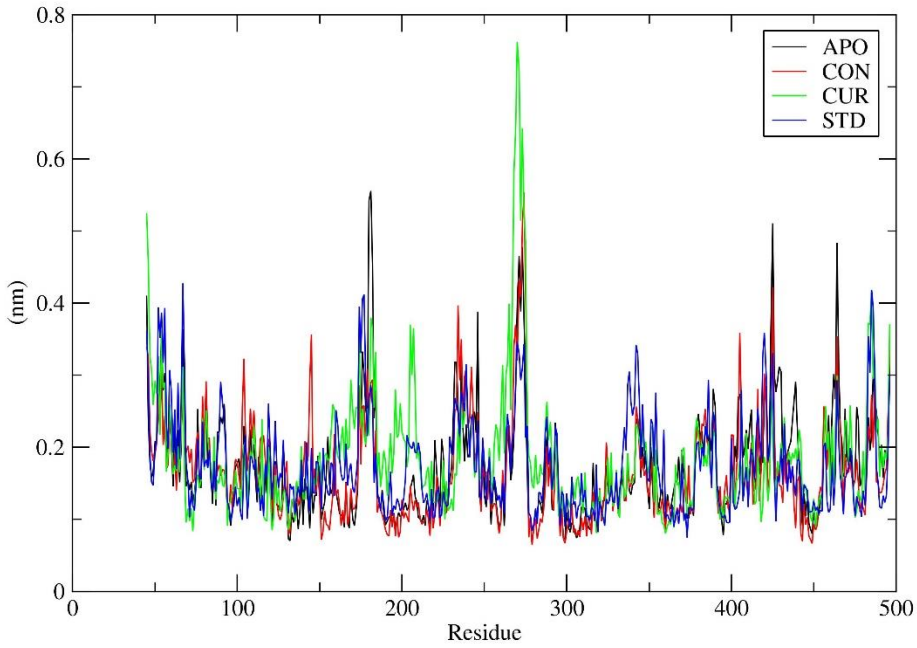

Figure 8. Study plot of RMSF of 3S7S-APO (Black), 3S7S-CON (Red), 3S7S-Curcumin (Green), and 3S7S-Standard (Blue) for 100 ns MD simulation.

Further, Rg of the complexes was also analyzed. Rg is the root mean square distance of the protein atoms from the axis of rotation [36]. It is one of the effective structural parameters for investigating the compactness and rigidity of the protein during the simulation. Rg values of backbone atoms of protein were plotted as a function of simulation time, as represented in Figure 9. The results show that the compounds did not cause significant structural alterations in the protein.

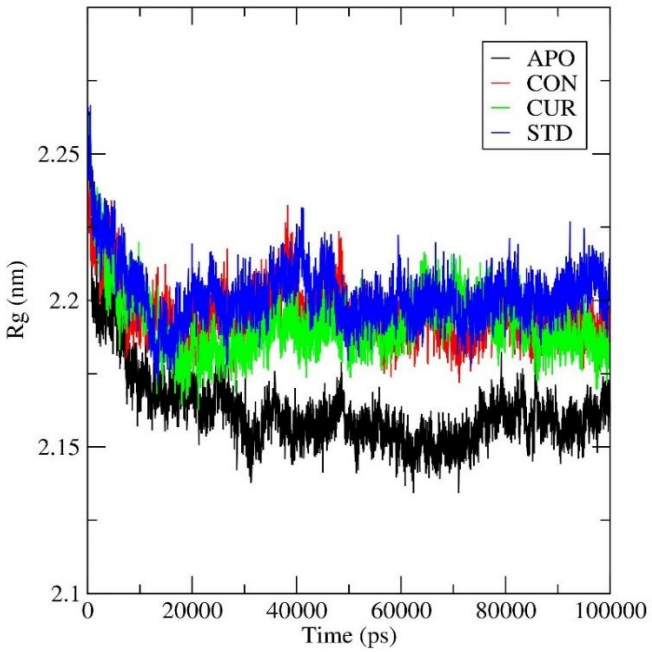

Figure 9. Study plot of the radius of gyration of 3S7S-APO (Black), 3S7S-CON (Red), 3S7S-Curcumin (Green), and 3S7S-Standard (Blue) for 100 ns MD simulation.

The SASA analysis was performed to determine how much the target protein was exposed to the solvent molecules around it during simulation [37]. The SASA values were

calculated and plotted as a function of time, as shown in Figure 10, to examine the changes in the surface area of protein. Based on the results, it was found that the surface area of the receptor protein in the complexes shrank during the simulation.

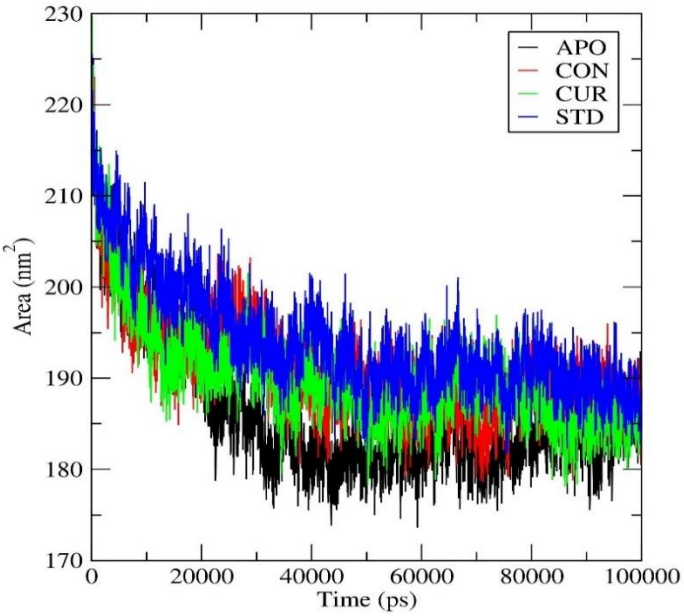

Figure 10. Study plot of the Solvent accessible surface area of 3S7S-APO (Black), 3S7S-CON (Red), 3S7S-Curcumin (Green), and 3S7S-Standard (Blue) for 100 ns MD simulation.

The binding affinity of ligands with the target protein was examined by analyzing the MD trajectories. The extent of hydrogen bond formation of the ligands with the receptor protein during the entire simulation was interpreted and depicted in Figure 11.

In the case of the CON-protein complex, the conjugate formed a good number of hydrogen bonds with aromatase protein with a maximum of six bonds at several time frames specifying stronger affinity towards the target. The stability of the complex is indicated by the consistent formation of almost three hydrogen bonds for the complete simulation time. For the curcumin complex, two hydrogen bonds were formed consistently, with a maximum of five bonds at certain periods. The standard exemestane formed two consistent hydrogen bonds with a maximum of three bonds at specific time intervals in the standard complex. The results signify that the conjugate has a pronounced affinity with the target protein.

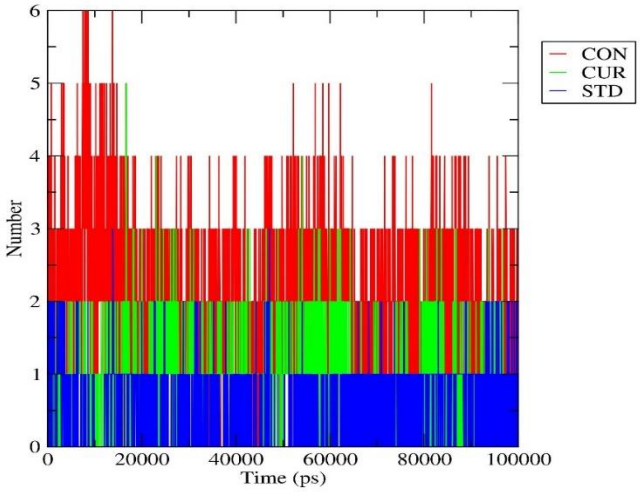

Figure 11. Study plot of Hydrogen bonds of 3S7S-CON (Red), 3S7S-Curcumin (Green), and 3S7S-Standard (Blue) for 100 ns MD simulation.

4. Conclusions

The hybrid conjugate of curcumin and metformin may synergistic anti-cancer activity with reduced toxicity. Molecular docking studies were performed to investigate the cytotoxic potential of curcumin-metformin conjugate compared with that of curcumin and metformin against breast cancer targets. Based on the docking studies, it can be concluded that the conjugate is predicted to have good cytotoxic activity. The conjugate was found to possess a maximum docking score (-9.7 Kcal/mol) against the human placental aromatase enzyme and shows more potent interactions with the target protein than curcumin and metformin. In addition, MD simulations indicate the stability of the receptor-ligand complex. Further *in vitro* and *in vivo* studies are needed to determine the effectiveness of curcumin-metformin conjugate.

Funding

This research received no external funding.

Acknowledgments

The authors are thankful to the Faculty of Pharmacy, M.S. Ramaiah University of Applied Sciences, for providing the facilities to carry out the research work.

Conflicts of Interest

The authors declare no conflict of interest.

References

1. Ferlay, J.; Colombet, M.; Soerjomataram, I.; Parkin, D.; Pineros, M.; Znaor, A. Cancer statistics for the year 2020: An overview. *International Journal of Cancer* **2021**, *149*, 778-789, https://doi.org/10.1002/ijc.33588.
2. Sung, H.; Ferlay, J.; Siegel, R.; Laversanne, M.; Soerjomataram, I.; Jemal, A. Global Cancer Statistics 2020: GLOBOCAN Estimates of Incidence and Mortality Worldwide for 36 Cancers in 185 Countries. *CA: A Cancer Journal for Clinicians* **2021**, *71*, 209-249, https://doi.org/10.3322/caac.21660.
3. Harbeck, N.; Penault-Llorca, F.; Cortes, J.; Gnant, M.; Houssami, N.; Poortmans, P. Breast cancer. *Nature Reviews Disease Primers* **2019**, *5*, https://doi.org/10.1038/s41572-019-0111-2.
4. Lima, S.; Kehm, R.; Terry, M. Global breast cancer incidence and mortality trends by region, age-groups, and fertility patterns. *EClinicalMedicine* **2021**, *38*, 100985, https://doi.org/10.1016/j.eclinm.2021.100985.
5. Paduraru, D.N.; Alexandra, B.; Ion, D.; Dumitrascu, M.C.; Nitipir, C.; Stoian, A.P.; Hainarosie, R.; Bolocan, A.; Orlov, C.; Badiu, D.C.; et al. Latest news and trends in what concerns the risk factors of endometrial cancer. *Romanian Biotechnological Letters* **2018**, *23*, 14056-14066.
6. Masuda, H.; Zhang, D.; Bartholomeusz, C.; Doihara, H.; Hortobagyi, G.N.; Ueno, N.T. Role of epidermal growth factor receptor in breast cancer. *Breast Cancer Research and Treatment* **2012**, *136*, 331-345, https://doi.org/10.1007/s10549-012-2289-9.
7. Li, T.F.; Zeng, H.J.; Shan, Z. Overexpression of kinesin superfamily members as prognostic biomarkers of breast cancer. *Cancer Cell International* **2020**, *20*, https://doi.org/10.1186/s12935-020-01191-1.
8. Guido, B.C.; Ramos, L.M.; Nolasco, D.O. Impact of kinesin Eg5 inhibition by 3,4-dihydropyrimidin-2(1H)-one derivatives on various breast cancer cell features. *BMC Cancer* **2015**, *283*, https://doi.org/10.1186/s12885-015-1274-1.
9. Mayer, E.L. Targeting breast cancer with CDK inhibitors. *Current Oncology Reports* **2015**, *17*, 443, https://doi.org/10.1007/s11912-015-0443-3.
10. Abdel-Magid, A.F. Potential of Cyclin-Dependent Kinase Inhibitors as Cancer Therapy. *ACS Medicinal Chemistry Letters* **2021**, *12*, 182-184, https://doi.org/10.1021/acsmedchemlett.1c00017.

11. Ghosh, D.; Lo, J.; Morton, D.; Valette, D.; Xi, J.; Griswold, J.; Hubbell, S.; Egbuta, C.; Jiang, W.; An, J.; Davies, H.M. Novel aromatase inhibitors by structure-guided design. *Journal of Medicinal Chemistry* **2012**, *55*, 8464-76, https://doi.org/10.1021/jm300930n.
12. Hua, H.; Zhang, H.; Kong, Q. Mechanisms for estrogen receptor expression in human cancer. *Experimental Hematology & Oncology* **2018**, *24*, https://doi.org/10.1186/s40164-018-0116-7.
13. Teiten, M.; Dicato, M.; Diederich, M. Hybrid Curcumin Compounds: A New Strategy for Cancer Treatment. *Molecules* **2014**, *19*, 20839-20863, https://doi.org/10.3390/molecules191220839.
14. Goel, A.; Kunnumakkara, A.; Aggarwal, B. Curcumin as "Curecumin": From kitchen to clinic. *Biochemical Pharmacology* **2008**, *75*, 787-809, https://doi.org/10.1016/j.bcp.2007.08.016.
15. Banik, U.; Parasuraman, S.; Adhikary, A.K.; Othman, N.H. Curcumin: The spicy modulator of breast carcinogenesis. *Journal of Exprimental & Clinical Cancer Research* **2017**, *36*, 1-16, https://doi.org/10.1186/s13046-017-0566-5.
16. Hu, S.; Xu, Y.; Meng, L.; Huang, L.; Sun, H. Curcumin inhibits proliferation and promotes apoptosis of breast cancer cells. *Experimental and Therapeutic Medicine* **2018**, *16*, 1266-1272, https://doi.org/10.3892/etm.2018.6345.
17. Anand, P.; Kunnumakkara, A.; Newman, R.; Aggarwal, B. Bioavailability of Curcumin: Problems and Promises. *Molecular Pharmaceutics* **2007**, *4*, 807-818, https://doi.org/10.1021/mp700113r.
18. Ireson, C.R.; Jones, D.J.; Orr, S.; Coughtrie, M.W.; Boocock, D.J,; Williams, M.L. Metabolism of the cancer chemopreventive agent curcumin in human and rat intestine. *Cancer Epidemiology, Biomarkers & Prevention* **2002**, *11*, 105-111, https://cebp.aacrjournals.org/content/11/1/105.short.
19. De, A.; Kuppusamy, G. Metformin in breast cancer: preclinical and clinical evidence. *Current Problems in Cancer* **2020**, *44*, 100488, https://doi.org/10.1016/j.currproblcancer.2019.06.003.
20. Dowling, R.J.; Niraula, S.; Chang, M.C. Changes in insulin receptor signaling underlie neoadjuvant metformin administration in breast cancer: a prospective window of opportunity neoadjuvant study. *Breast Cancer Research* **2015**, *17*, 32, https://doi.org/10.1186/s13058-015-0540-0.
21. Dowling, R.J.; Goodwin, P.J.; Stambolic, V. Understanding the benefit of metformin use in cancer treatment. *BMC Medicine* **2011**, *9*, 33, https://doi.org/10.1186/1741-7015-9-33.
22. Hirsch, H.A.; Iliopoulos, D.; Tsichlis, P.N.; Struhl, K. Metformin selectively targets cancer stem cells, and acts together with chemotherapy to block tumor growth and prolong remission. *Cancer Research* **2009**, *69*, 7507-7511, https://doi.org/10.1158/0008-5472.CAN-09-2994.
23. Jain, S.; Gill, M.S.; Pawar, H.S.; Suresh, S. Novel Curcumin Diclofenac Conjugate Enhanced Curcumin Bioavailability and Efficacy in Streptococcal Cell Wall-induced Arthritis. *Indian Journal of Pharmaceutical Sciences* **2014**, *76*, 415-422, https://www.ncbi.nlm.nih.gov/pmc/articles/PMC4243258/.
24. Berman, H.M.; Westbrook, J.; Feng, Z.; Gilliland, G.; Bhat, T.N.; Weissig, H.; Shindyalov, I.N.; Bourne, P.E. The Protein Data Bank. *Nucleic Acids Research* **2000**, *28*, 235-42, https://doi.org/10.1093/nar/28.1.235.
25. Dallakyan, S.; Olson, A.J. Small-molecule library screening by docking with PyRx. *Methods in Molecular Biology* **2015**, *1263*, 243-50, https://doi.org/10.1007/978-1-4939-2269-7_19.
26. Gaillard, T. Evaluation of AutoDock and AutoDock Vina on the CASF-2013 benchmark. *Journal of Chemical Information and Modeling* **2018**, *58*, 1697-1706, https://doi.org/10.1021/acs.jcim.8b00312.
27. Kalimuthu, A.K.; Panneerselvam, T.; Pavadai, P. Pharmacoinformatics-based investigation of bioactive compounds of Rasam (South Indian recipe) against human cancer. *Scientific Reports* **2021**, *11*, https://doi.org/10.1038/s41598-021-01008-9.
28. Adeniji, S.E.; Arthur, D.E.; Oluwaseye, A. Computational modeling of 4-Phenoxynicotinamide and 4-Phenoxypyrimidine-5-carboxamide derivatives as potent antidiabetic agent against TGR5 receptor. *Journal of King Saud University - Science* **2020**, *32*, 102-115, https://doi.org/10.1016/j.jksus.2018.03.007.
29. Jia, C.Y.; Li, J.Y.; Hao, G.F.; Yang, G.F. A drug-likeness toolbox facilitates ADMET study in drug discovery. *Drug Discovery Today* **2020**, *25*, 248-258, https://doi.org/10.1016/j.drudis.2019.10.014.
30. Lindahl, E.; Abraham, M.J.; Hess, B.; van der Spoel. *GROMACS 2021.3 Manual* **2021**. https://doi.org/10.5281/zenodo.5053220.
31. Zai, Y.; Xi, X.; Ye, Z.; Ma, C.; Zhou, M. Aggregation and Its Influence on the Bioactivities of a Novel Antimicrobial Peptide, Temporin-PF, and Its Analogues. *International Journal of Molecular Sciences* **2021**, *22*, 4509, https://doi.org/10.3390/ijms22094509.
32. Krishna, S.; Kumar, S.B.; Murthy, T.P.K.; Murahari, M. Structure-based design approach of potential BCL-2 inhibitors for cancer chemotherapy. *Computers in Biology and Medicine* **2021**, *134*, 104455, https://doi.org/10.1016/j.compbiomed.2021.104455.

33. Van Aalten, D.; Bywater, R.; Findlay, J.B.C. PRODRG, a program for generating molecular topologies and unique molecular descriptors from coordinates of small molecules. *Journal of computer-aided molecular design* **1996**, *10*, 255-262, https://doi.org/10.1007/BF00355047.
34. Kumari, R.; Kumar, R.; Lynn, A. g-mmpbsa -A GROMACS tool for high-throughput MM-PBSA calculations. *Journal of Chemical Information and Modeling* **2014**, *54*, 1951–1962, https://doi.org/10.1021/ci500020m.
35. Odabasoglu, H.; Erdogan, T.; Karci, F. Synthesis & characterization of heterocyclic disazo - azomethine dyes and investigating their molecular docking & dynamics properties on acetylcholine esterase (AChE), heat shock protein (HSP90α), nicotinamide N-methyl transferase (NNMT) and SARS-CoV-2 (2019-nCoV, COVID-19) main protease (Mpro). *Journal of Molecular Structure* **2021**, *1252*, 131974, https://doi.org/10.1016/j.molstruc.2021.131974.
36. Rahman, M.M.; Saha, T.; Islam, K.J.; Suman, R.H. Virtual screening, molecular dynamics and structure-activity relationship studies to identify potent approved drugs for Covid-19 treatment. *Journal of Biomolecular Structure and Dynamics* **2021**, *16*, 6231-6241, https://doi.org/10.1080/07391102.2020.1794974.
37. Al-Karmalawy, A.A.; Dahab, M.A.; Metwaly, A.M.; Elhady, S.S. Molecular Docking and Dynamics Simulation Revealed the Potential Inhibitory Activity of ACEIs Against SARS-CoV-2 Targeting the hACE2 Receptor. *Frontiers in Chemistry* **2021**, *9*, 227, https://doi.org/10.3389/fchem.2021.661230.